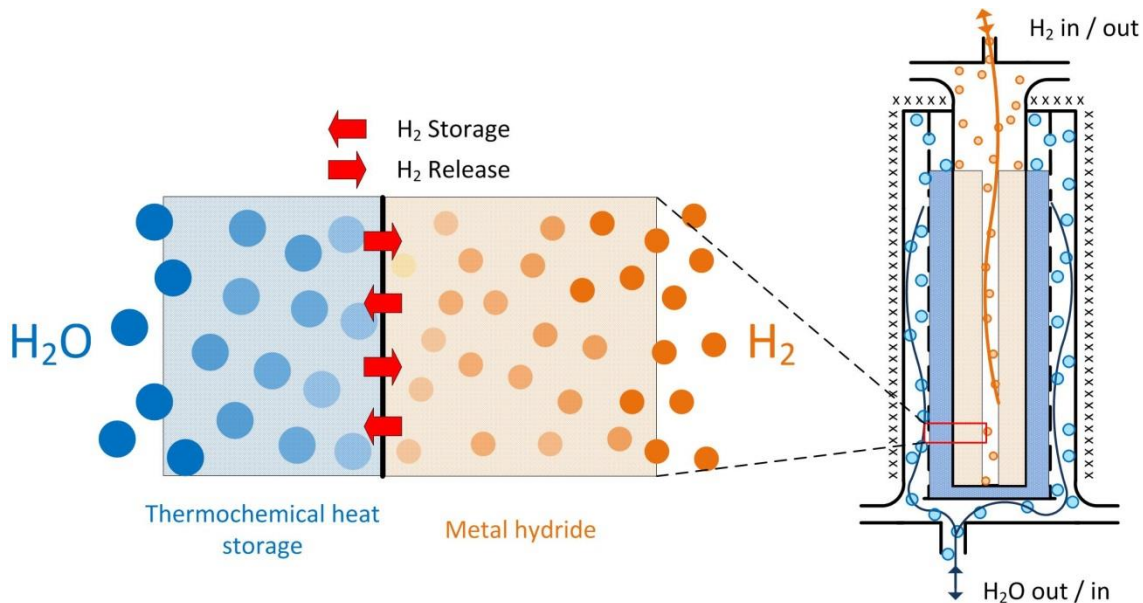


# High capacity, low pressure hydrogen storage based on magnesium hydride and thermochemical heat storage: Experimental proof of concept

Michael Lutz\*, Marc Linder, Inga Bürger

Institute of Engineering Thermodynamics, German Aerospace Center (DLR), Pfaffenwaldring 38-40  
D-70569 Stuttgart, Germany

\*Corresponding author; e-mail: [michael.lutz@dlr.de](mailto:michael.lutz@dlr.de)



Abstract:

With hydrogen becoming more and more important as energy carrier, there is a need for high capacity storage technologies preferably operating at low pressures. Chemical storage in metal hydrides is promising for that purpose, but they require thermal management for hydrogen release and storage, respectively. To overcome this challenge, it is beneficial to store the heat needed for hydrogen release during hydrogen storage in the storage system keeping the additional effort to provide that heat low. In this work, the experimental proof of concept of an adiabatic storage reactor is presented. Magnesium hydride and magnesium hydroxide have been used for hydrogen storage and thermochemical heat storage, respectively. A prototype reactor has been developed and experimentally investigated. It was found that the operating temperature of the materials can be adjusted with the gas pressure in a way to establish a temperature gradient from the  $\text{MgH}_2$  to the  $\text{Mg}(\text{OH})_2$  and vice versa. Hydrogen storage and release is enhanced by the thermochemical heating/cooling. A pressure of 9 bar is sufficient to store hydrogen with a capacity of  $20.8 \text{ g}_{\text{H}_2} \text{ L}^{-1}$  based on the two materials only, without the steel vessel or insulation. In the heat storage compartment,  $300 \text{ }^\circ\text{C}$  have been reached at 9.75 bar during heat release which is high enough to drive the  $\text{MgH}_2$  dehydrogenation.

Keywords:

Hydrogen storage, thermochemical heat storage, magnesium hydride, magnesium hydroxide

Highlights:

- Experimental hydrogen storage and release from a novel adiabatic storage reactor
- Coupling of a metal hydride with a thermochemical heat storage material
- Magnesium hydride and magnesium hydroxide suitable for hydrogen storage
- Magnesium oxide hydration at 9.75 bar results in reactor temperature of 300 °C

## Introduction

For a successful transformation of the global energy systems towards renewable energy there is a need for large scale energy storage. Storing energy chemically in the form of hydrogen is beneficial, since hydrogen can be combusted, transported or used as a precursor for other chemical compounds, such as power-to-gas [1]. Hence, there is an increasing need for efficient hydrogen storage. State of the art hydrogen storage technologies, such as liquefaction or pressurized storage, lack efficiency, pose safety threats or have low storage densities. Additionally, political regulations have to be taken into account. In Japan, a country leading in hydrogen technologies, extensive and expensive safety measures have to be installed if hydrogen is stored above 10 bar in housing environments [2] [3]. Therefore, it would be beneficial to store hydrogen at a pressure as low as possible. This is challenging due to its low density at ambient pressure and 273 K of  $0.08988 \text{ g L}^{-1}$  [4].

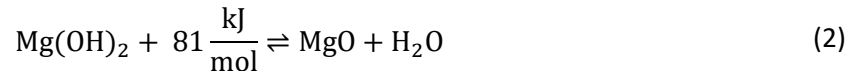
Thermochemical systems have the advantage that the hydrogen is not stored in its elementary form, but within liquid [5] or solid chemical compounds [6]. With these systems, higher volumetric densities can be achieved than in gaseous storage. Metal hydrides have been studied intensively for that purpose [4]. The challenge of utilizing metal hydrides and other thermochemical systems is their heat of reaction which has to be managed. This is especially challenging with increasing reaction temperatures. One example of a promising thermochemical system is based on the reversible formation of magnesium hydride. However, as its operating temperature is at around  $300 \text{ }^\circ\text{C}$ , the thermal management becomes difficult, especially the low-cost supply of thermal energy at that temperature level. An option to overcome this disadvantage is to store the heat during hydrogen absorption in a way that it is available for the hydrogen release. Heat storage and release have to take place at a temperature level fitting to the reaction temperature of the metal hydride. Using a phase change material operating in that temperature range for that purpose has been investigated before [7] [8]. Intrinsically, the temperature levels of heat storage and release are identical for the PCM, which is its melting point. However, it would be beneficial if the temperature level of heat storage is lower than the temperature level of the heat release. Thermochemical heat storage material utilizing a gas-solid reaction exhibit this feature, because the gas pressure can be adjusted. This is why in the present work the combination of magnesium hydride, as a high temperature metal hydride, with magnesium hydroxide as thermochemical heat storage is investigated experimentally for stationary, centralized hydrogen storage, which may have advantages over decentralized systems [9].

The main idea of the so-called adiabatic storage concept is the combination of an exothermal reaction with an endothermal one compensating for each other. Therefore, the reactor can be operated with minimal heat management, since the heat of reaction during hydrogen storage is available for the hydrogen release making it adiabatic to the environment. Compared to heat storage in a PCM, the usage of the thermochemical heat storage material yields in higher storage densities [10] and in an additional degree of freedom, since the reaction temperature can be adjusted with the gas pressure.

Magnesium, which is non-toxic [11] and abundantly available, is the main compound of both reactions. In this study, magnesium hydride is used for hydrogen storage [12].



The heat of reaction is stored in the Mg(OH)<sub>2</sub> / MgO system.



For hydrogen storage, the heat of absorption is conducted to the Mg(OH)<sub>2</sub> bed, where the heat is consumed by its dissociation to MgO and H<sub>2</sub>O. For the heat transfer to emerge, the temperature in the MgH<sub>2</sub> bed has to be higher than the temperature in the Mg(OH)<sub>2</sub> bed. For hydrogen release, water vapor has to be supplied to the MgO bed. The previously stored thermal energy is released and transferred to the MgH<sub>2</sub> bed. Hence, the temperature gradient has to be reversed. The feasibility of this system has been investigated analytically [13] before. Thereafter, a numerical study for hydrogen storage [14] and hydrogen release [15] was conducted. A more detailed description of the system can be found there. In this work the experimental proof of concept of this new hydrogen storage reactor is presented.

Besides cost [16], the volumetric storage density and the pressure level are important parameters for stationary hydrogen storage systems. The pressure level may translate directly into cost if safety regulations are regarded. Additional incorporation of the thermochemical heat storage material results in a heavier system compared to the metal hydride alone, but for stationary application the weight of the system is not that important. Additionally, the energy being required to compress hydrogen to that pressure for storage, which is 15% of its lower heating value in the 700 bar case [18], has not to be brought up, improving the systems overall efficiency significantly. Furthermore, in contrast to compressed hydrogen storage systems, the adiabatic storage reactor impedes the hydrogen release by itself in case of a leak. This is due to the endothermic nature of the hydrogen release.

To reach a sufficiently high temperature level in the MgO compartment for the dehydrogenation of Mg<sub>90</sub>Ni<sub>10</sub> and drive the hydrogen release reaction, approximately 10 bar of water vapor are required. There are two options to provide this water vapor. Suppose, the hydrogen is used in a high temperature PEM fuel cell operating at 180 °C, the waste heat of such a fuel cell can be used to evaporate water from an external tank at a pressure of 10 bar. Approximately 40% of the HT-PEM's waste heat is sufficient to heat liquid water from 20 °C to 180 °C and to evaporate it at 180 °C. A more detailed analysis of this systems integration can be found in [15]. Another option is to directly use the fuel cell's exhaust gas, which contains water vapor, and feed it to the MgO compartment after compression to 10 bar. Both options would be feasible in case of stationary hydrogen storage.

In this work, a prototype reactor for stationary hydrogen storage was developed and tested. First the experimental setup is presented, followed by the experimental characterization of the system. Afterwards, starting points for optimization and a summary are shown.

## Experimental setup

The adiabatic storage concept utilizes two thermochemical reactions involving hydrogen and water vapor. Therefore, the experimental test bench consists of three main components – The water vapor infrastructure, the hydrogen infrastructure and the prototype reactor. The whole setup is shown in Figure 1.

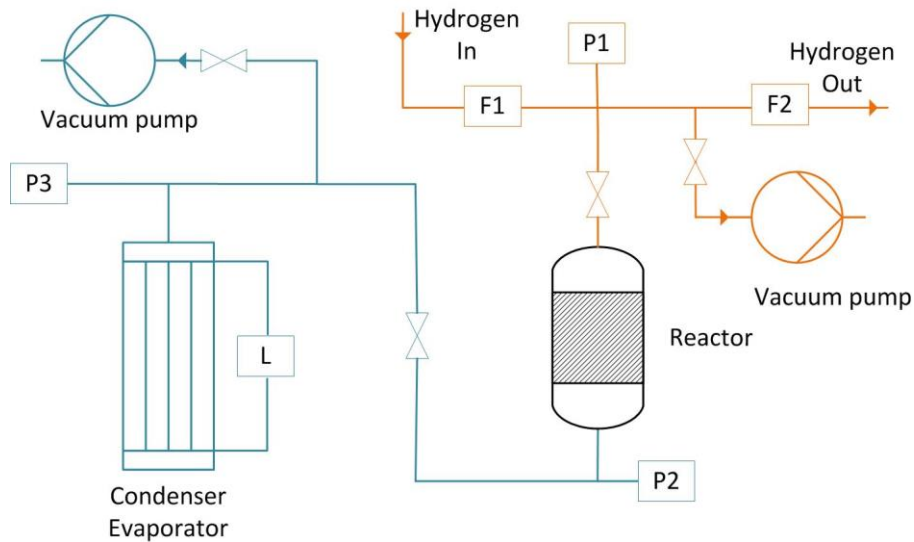


Figure 1 - Test bench schematic; Hydrogen- and water vapor infrastructure orange and blue, respectively; F: Flow meter; P: Pressure sensor; L: Level meter.

### Water vapor infrastructure

Water vapor is supplied or withdrawn from the reactor with a tube bundle heat exchanger acting as evaporator or condenser, respectively. The heat exchanger is tempered with thermal oil while its water side is closed to the environment. That's why with adjustment of the oil temperature, the water vapor pressure in the heat exchanger and, thus, in the reactor can be controlled. It has been demonstrated that thermochemical reactions can be supplied with water vapor using this system [19]. The present setup allows for water vapor pressures from 50 mbar to 10 bar, which corresponds to oil temperatures from 33 °C to 180 °C. The evaporator/condenser is equipped with a guided wave radar level meter (VEGAFLEX 81, VEGA Grieshaber KG,  $\pm 2$  mm) measuring the level of the liquid water in the tube bundle. The change in level corresponds directly to the water uptake/release from the thermochemical reaction. Hence, the reacted fraction of the thermochemical reaction can be calculated from the level change. The pressure in the reactor was measured by the pressure sensor P2 (Cerabar M PMP55, Endress+Hauser Messtechnik GmbH+Co.KG,  $\pm 0.15\%$ ) as shown in Figure 1.

### Hydrogen infrastructure

Hydrogen can be supplied- or withdrawn from the reactor using the volume-flow-controllers F1 (F-232MI, Bronkhorst High-Tech B.V.,  $\pm 0,5\%$  Rd plus  $\pm 0,1\%$  FS) and F2 (F-111AI, Bronkhorst High-Tech B.V.,  $\pm 0,8\%$  Rd plus  $\pm 0,2\%$  FS). Minimal hydrogen flow rates are  $4.3 \text{ g h}^{-1}$  and  $2.7 \text{ g h}^{-1}$  for inflow and outflow, respectively.

The operating pressure ranges from 1 bar to 50 bar and is measured with pressure sensor P1 (PA-21Y, KELLER AG,  $\pm 0.4$  bar). The controllers can either be operated sustaining a constant volume flow rate or a constant pressure.

### Materials and Prototype reactor

For the metal hydride, an alloy of 90% Magnesium and 10% Nickel was used. The  $Mg_{90}Ni_{10}$  alloy was melt-spun, mixed with 10 wt.% expanded natural graphite and compressed to pellets with 30 mm diameter at 300 MPa. A central hole with 5 mm diameter was drilled through the pellet to allow for hydrogen distribution and insertion of thermocouples. These pellets were manufactured at Fraunhofer Institute for Manufacturing Technology and Advanced Materials IFAM in Dresden, Germany [20]. For the thermochemical heat storage material, magnesium hydroxide  $Mg(OH)_2$  was obtained from Sigma-Aldrich (Nr. 63081), which is an unmodified, fine, white powder.

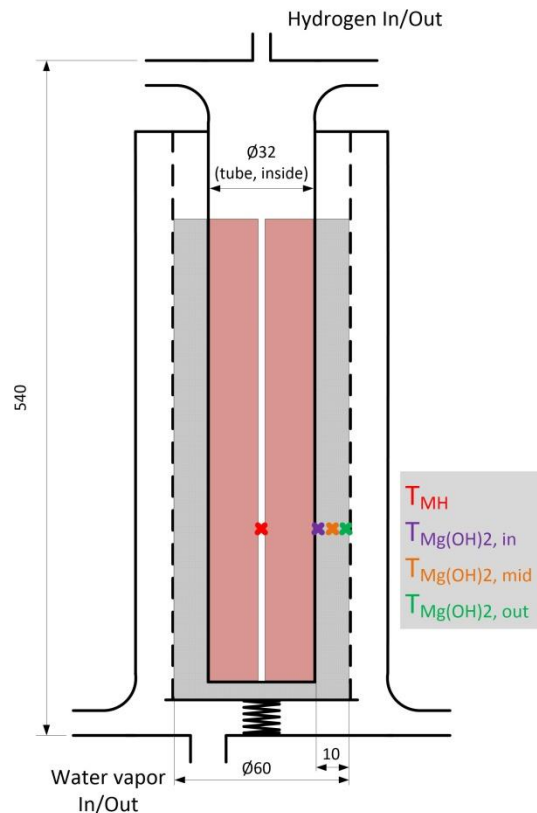


**Figure 2 - Reactor schematic including thermocouples;  $Mg_{90}Ni_{10}$  (red);  $Mg(OH)_2$  (grey); Dashed line: Sinter metal filter; Dimensions in mm; Not to scale; Inner tube's wall thickness: 4 mm.**

The prototype reactor is displayed in detail in Figure 2. It consists of a double tube with 234 g  $Mg_{90}Ni_{10}$  (red) in the inner tube and 400 g  $Mg(OH)_2$  (grey) in the outer tube. With a gravimetric hydrogen capacity of 5.3 wt. % for the  $Mg_{90}Ni_{10}$  pellets, the amount of metal hydride was chosen in a way that approximately 12 g hydrogen can be stored. To take up the heat of absorption, 400 g  $Mg(OH)_2$  are needed assuming that 84% of the  $Mg(OH)_2$  react. Several thermocouples (Type K,  $\pm 1.5$  °C) are incorporated into the reactor. For clarity, only the thermocouples that are referenced in the results section are shown in Figure 2. These

thermocouples are on the same height, the ones in the  $\text{Mg}(\text{OH})_2$  section are slightly offset along the circumference. Due to large flanges at both ends of the reactor, the height of the thermocouple's positions was chosen to be at a position the least thermal losses were assumed. Since the  $\text{Mg}_{90}\text{Ni}_{10}$  pellets have a central hole and the  $\text{Mg}(\text{OH})_2$  powder is kept in place with a sinter metal filter, diffusion pathways for the hydrogen and water vapor are 10 mm and 13 mm, respectively. Therefore, mass transfer limitations can be excluded.

### Experimental procedure and evaluation

For hydrogen storage, the adiabatic storage reactor was completely depleted of hydrogen before the initiation of the hydration experiment. For that purpose the  $\text{Mg}_{90}\text{Ni}_{10}$  was repeatedly exposed to vacuum until the temperatures didn't decline anymore. The  $\text{MgO}/\text{Mg}(\text{OH})_2$  was exposed to the water vapor for several hours until no further change in temperatures has been measured indicating that the hydration is complete. The system's components were tempered to the desired temperatures, which may be different for separate experiments. The initial temperatures are reported at the respective analysis section. It was chosen to be not too high, because a heat-up of the bed due to the exothermal reaction should be observed. It should not be too low as well, since the majority of the exothermally released heat should drive the endothermal reaction and not only heat-up the bed. At the same time, the dehydration of  $\text{Mg}(\text{OH})_2$  should not take place at the initial temperature. The selected initial temperatures comply with these criteria. The reaction was initiated by increasing the hydrogen pressure to the desired value. Accordingly, for hydrogen release, the adiabatic storage reactor was fully loaded with hydrogen before the experiment. It was ensured with the increase of the hydrogen pressure at least 15 bar above the equilibrium pressure, waiting until the temperatures levelled off and no further pressure decrease in the closed reactor could be observed. Full dehydration of the  $\text{Mg}(\text{OH})_2$  before the experiment's initiation was ensured with additional heat up using the external heating and application of vacuum until the temperatures levelled off. The hydrogen release reaction was initiated by a sudden increase in water vapor to the desired value and setting the desired hydrogen volume flow rate in the mass flow controller.

The reactor is heated with an external heating wire to the initial temperature. During the course of the experiments this external heating was kept turned on to compensate for thermal losses. For the experimental evaluation it is important that the endothermal thermochemical reaction is not driven by input of thermal energy from the external heating wire, but from the thermal energy by the exothermal reaction. This is the case if the temperature levels in the reactor are higher during the experiment than before starting it. Unless stated otherwise this was the case in all presented experiments.

The conversion of the thermochemical heat storage reaction is monitored by the change of the liquid level in the evaporator/condenser. The level-meter works with guided wave radar. Therefore, its signal is subject to fluctuations if the liquid surface is uneven which is the case during evaporation and condensation. Rapid jumps in the signal in both directions have been observed during condensation. Since they do not have a physical meaning, they have been disregarded. For evaluation, the signal from the level meter had to be smoothed. That is why in the result section, the conversion calculations are shown for the compensated and smoothed data as well as the raw, non-smoothed data.

The reacted fractions of the materials have been calculated based on the maximum experimental possible conversion. For the  $\text{Mg}_{90}\text{Ni}_{10}$ , 100% of reacted fraction corresponds to 12.4 g of hydrogen uptake/release. For the  $\text{Mg}(\text{OH})_2$ , it was experimentally determined that approximately 80% of the filled in  $\text{Mg}(\text{OH})_2$  reacts. This value was obtained during the first heat-up of the  $\text{Mg}(\text{OH})_2$  filled into the reactor. Therefore, the material was dehydrated and the water was condensed in the evaporator/condenser until no further condensation was observed. From the amount of condensed water, the reacted fraction was calculated. This is why 99 g water uptake/release represents 100%.

## Hydrogen storage

Previous analytical calculations indicated that with the present materials, hydrogen storage in the adiabatic storage reactor is possible at 10 bar hydrogen pressure or below [13]. In this section the hydrogen storage properties of the reactor prototype are evaluated. During hydrogen storage, the metal hydride reacts with hydrogen which takes place in the inner tube and is the exothermal reaction. The endothermal reaction happening in the outer tube is the dissociation of  $\text{Mg}(\text{OH})_2$ . For successful hydrogen storage, the temperature in the metal hydride has to be higher than the temperature in the thermochemical heat storage material for a temperature gradient to be established.

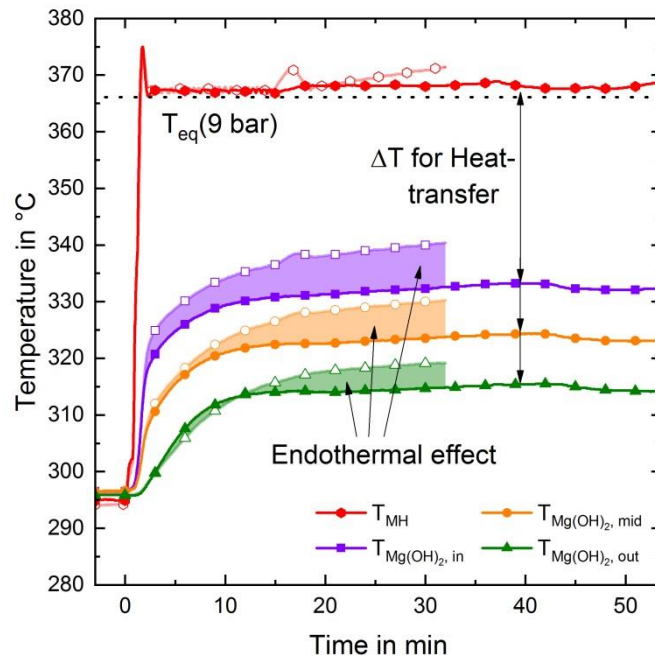


Figure 3 - Reactor temperatures during hydrogen storage at 9 bar hydrogen pressure and 60 mbar water vapor partial pressure; Open markers: Reference experiment; Full markers: Combined experiment; Thermocouple positions in Figure 2.

To evaluate the influence of the thermochemical heat storage material on the reactor's performance during hydrogen absorption, a reference experiment was conducted at which only the magnesium hydride was active. The heat storage material did not participate since it was present as  $\text{MgO}$  which is inert at these conditions. This experiment is shown with open markers in Figure 3. Both experiments were started with a pressure increase to 9 bar hydrogen. It can be seen that the temperature in the magnesium hydride (red) rises sharply to the theoretical equilibrium temperature. Heat transfer into the inert  $\text{MgO}$  bed takes place and subsequently, temperatures rise as well and a temperature gradient can be observed since the thermocouples are placed in different bed-depths (see Figure 2). For the combined experiment, the thermochemical heat storage material  $\text{Mg}(\text{OH})_2$  dissociates endothermally into  $\text{MgO}$  and water vapor. While the temperature course for the magnesium hydride is the same for the first 15 minutes, the

temperatures in the magnesium hydroxide are lower than during the reference experiment. This behavior proves that the  $\text{Mg(OH)}_2$  starts to dissociate, creating a heat sink.

Furthermore, after 15 minutes, the operating mode was changed from pressure control to flow rate control. At approximately 15 minutes the flow rate into the reactor was set to  $4.3 \text{ g h}^{-1}$ . The temperature (and pressure, not displayed) starts to rise. Hence, the hydrogen absorption rate of the reactor from that moment on is below  $4.3 \text{ g h}^{-1}$ . In the combined experiment this is the case after approximately 50 min. Subsequently, more hydrogen can be stored in less time.

Overall, it is evident that the temperature of the metal hydride sticks to the equilibrium temperature for the displayed time frame, indicating that here the limiting reaction is the dehydration of  $\text{Mg(OH)}_2$ . The hydrogenation reaction could proceed faster in case the heat of reaction would be removed more quickly by the thermochemical heat sink.

#### Influence of temperature level on the hydrogen storage process

The reaction temperature is a crucial factor in every chemical reaction. According to the Arrhenius law higher temperatures yield in faster reaction rates. In order to evaluate the influence of the reactor temperature on the hydrogen storage process, the initial temperature was increased by 50 K. To draw conclusion on the reaction kinetics, the temperature difference, and thus, heat-transfer between the reactive beds was aimed to be identical in both cases. Hence, hydrogen absorption pressure was also increased to 25.7 bar. The temperature difference during operation was estimated to be 45 K, as it can be seen in Figure 4 (A). In both cases, the magnesium hydride (red) reacts quickly to the respective equilibrium conditions. During hydrogen absorption the pressure was kept constant throughout the absorption. In both cases, the magnesium hydride temperature starts to decrease at around 62 min. Since the pressure did not change, the materials' reaction rate decreases – probably due to getting close to the full capacity. Viewing the temperature course in the magnesium hydroxide (orange), it is evident, that at the lower temperature, it is rather flat after an initial heat-up. At the higher temperature, the initial heat-up is less pronounced. Instead, the material slowly heats up to a maximum. Only at the maximum the temperature difference matches the temperature difference with the comparison-process. Before that, it is even higher which indicates an increased reaction rate in the endothermic  $\text{Mg(OH)}_2$  dehydration in the experiment at the higher temperature level. This can be confirmed by viewing the course of the reacted fraction in Figure 4 (B). At the same time, the reaction rate in the exothermic  $\text{H}_2$  absorption is significantly enhanced, indicating that the reactive heat sink in the  $\text{Mg(OH)}_2$  is more active.

In contrast to the initial temperature of  $295 \text{ }^\circ\text{C}$ , in this experiment the  $\text{Mg(OH)}_2$  is able to dehydrate at  $345 \text{ }^\circ\text{C}$ , which is why the initial pressure in the compartment was higher at the higher temperature. At the beginning of the process, the valve to the tempered condenser was opened, and the desired set pressure was reached quickly while only a small fraction of the materials reacted. Therefore, the first few minutes of the hydrated fraction are not shown in Figure 4 (B). The  $\text{Mg(OH)}_2$  dehydration rate slows down with

time. This is in agreement with the temperature course, since the temperature (orange, open markers) is rising slowly which means that less heat is consumed. At its maximum the same temperature difference

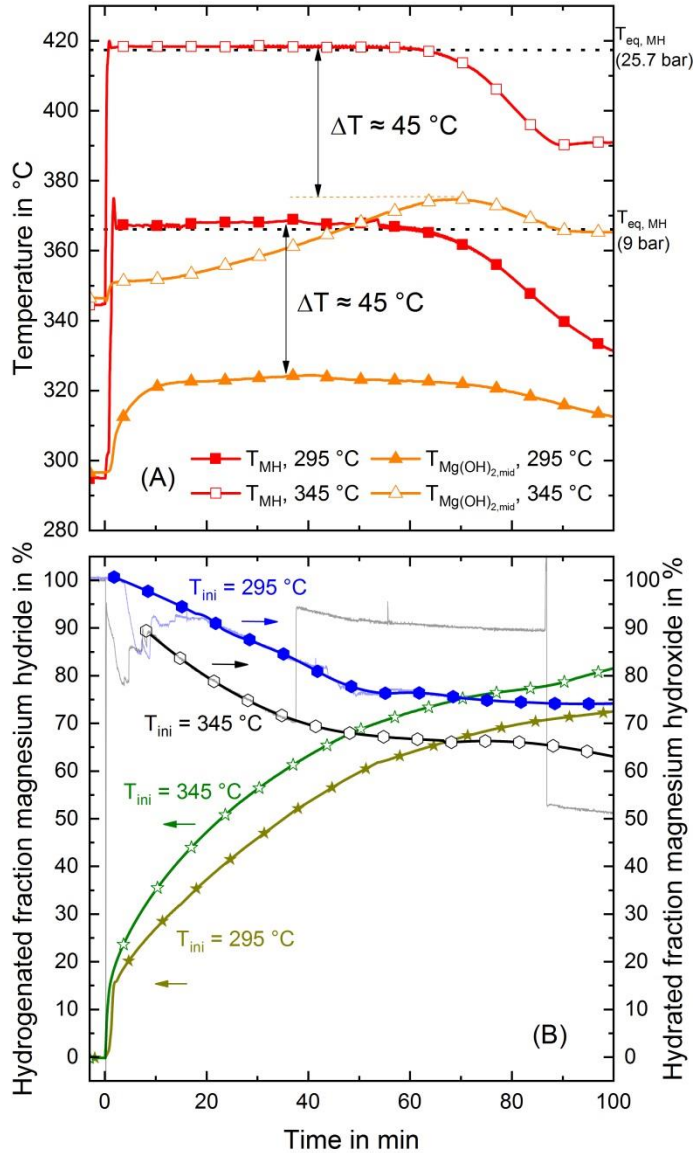


**Figure 4 - Influence of the temperature level; 60 mbar water vapor partial pressure; Open markers: Initial temperature 345 °C; Full markers: Initial temperature 295 °C; Light blue and grey lines: Original, unsmoothed data.**

of 45 K is reached as in the comparison process, indicating that the same reaction rate is reached in the two cases.

In Figure 4 (B) it can be seen that the conversions of the hydrogen storage – and heat storage reaction do not correspond to each other. In the 295 °C case, 73% of the  $MgH_2$  have reacted while only 26% of the  $Mg(OH)_2$  has been dehydrated after 100 min. In the 345 °C case it is similar with 81% and 36%, respectively. The amount of materials has been chosen in a way that corresponding conversions could be expected.

However, the heat of hydrogen absorption is not completely consumed by the endothermic  $\text{Mg(OH)}_2$  dehydration since thermal losses to the environment are present. With the  $\text{H}_2$  pressure increasing to the desired value, the temperature level in the reactor increases by 75 K. Therefore, not only a temperature gradient to the  $\text{Mg(OH)}_2$  bed, but also to the environment is established and thermal losses cannot be avoided in this small, single tube prototype reactor. In a larger system though, thermal losses will be a minor issue since the majority of the material will be in an inner bulk being more adiabatic, rather than on the outside of the storage reactor.

It can be concluded here, that with a higher temperature level in the reactor, faster hydrogen storage can be achieved. Since the equilibrium conditions are met almost instantly in both cases, the  $\text{Mg}_{90}\text{Ni}_{10}$  hydrogenation in the prototype reactor is not limited by mass transfer or its kinetics but by heat transfer. It would be able to react even faster if the heat of reaction would be withdrawn more effectively. A larger heat sink, like the acceleration of the  $\text{Mg(OH)}_2$  dehydration, would be beneficial for that purpose. Increasing the temperature level has this effect. Overall it can be concluded that in the present setup the  $\text{Mg(OH)}_2$  dehydration rate is the limiting factor for the hydrogen absorption process.

#### Influence of water vapor pressure and hydrogenation pressure

The adiabatic storage reactor is a complex system with several parameters, such as operating temperatures or gas pressures, being tunable to enhance the hydrogen storage process. In Figure 5, the influence of the water vapor condensation pressure and hydrogen storage pressure are shown. To eliminate influences of the startup procedure, the reaction progress from 2 min to 30 min is shown for various operation conditions. Two minutes after the start of hydrogen absorption, the pressure has adjusted to the desired value and  $\text{MgH}_2$  temperatures are in steady-state. For every case, the change in the reacted fraction is shown with 100% being the maximum achievable reacted fraction. For comparison, the reference experiment discussed in Figure 3 is included as well. The blue and orange bars in Figure 5 represent the reacted fraction of the  $\text{Mg(OH)}_2$  and  $\text{Mg}_{90}\text{Ni}_{10}$ , respectively. Ideally, the reacted fractions would be identical since the amount of material was chosen to compensate for each other. Thus, if there were no thermal losses, the heat being released by the exothermic hydrogenation would be consumed by the endothermic dehydration one-to-one and the reacted fractions would be the same. For the reference experiment, which was discussed in detail in Figure 3, there was no endothermic dehydration, as the material was present as inert  $\text{MgO}$ .

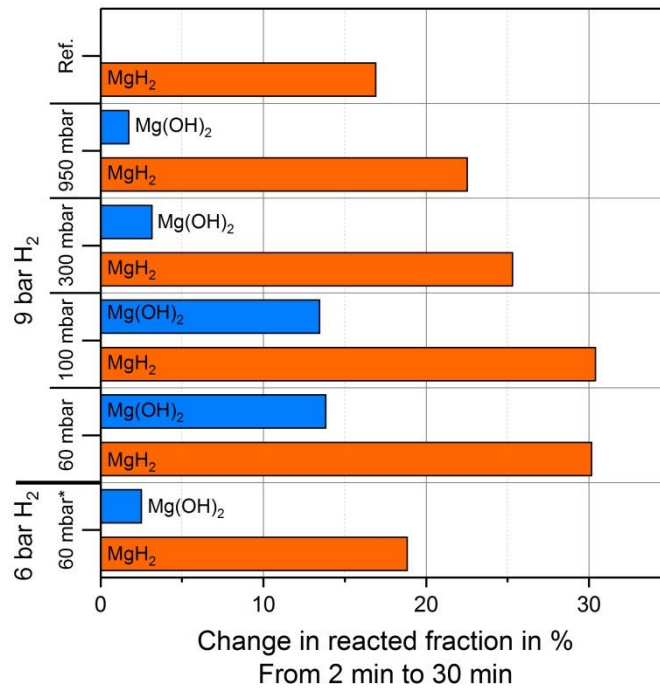


Figure 5 – Influence of water vapor condensation pressure and hydrogen pressure on hydrogen storage process; To avoid influences of the startup procedure, the timeframe for 2 min to 30 min is shown; Ref.: Reference experiment with inert heat storage material.

It is obvious that the water vapor condensation pressure influences the reaction rate. The difference in the reacted fractions between 60 mbar and 100 mbar is marginal, a clear difference to 300 mbar and 950 mbar can be seen, where significantly less  $\text{Mg(OH)}_2$  has reacted. This indicates that the increased water vapor pressure slows down the reaction. With the heat source of the  $\text{MgH}_2$  being the same, this can be attributed to reduced kinetics of the  $\text{Mg(OH)}_2$  dehydration. As it is the nature of gas-solid reactions, increased pressure of the gaseous reactant reduces the dissociation reaction rate. In the present experiment, this effect leads to less thermochemical cooling and therefore, less hydrogen storage. Concluding here, for fast hydrogen storage, the water vapor condensation pressure should be kept as low as possible, but a reduction from 100 mbar to 60 mbar does not have a significant effect on the hydrogen uptake. At 100 mbar, which corresponds to a  $\text{H}_2\text{O}$  condensation temperature of 46 °C, heat release to the ambient would still be possible.

Additionally, it can be seen that the hydrogen pressure of 6 bar compared to 9 bar reduces the reaction rate for both materials significantly. Even though the equilibrium temperature is also reached instantly at 6 bar for the  $\text{Mg}_{90}\text{Ni}_{10}$ , the overall temperature level is lower since its equilibrium temperature is only 348 °C, compared to 366 °C at 9 bar. That temperature is too low for the  $\text{Mg(OH)}_2$  dehydration to take place at a sufficiently fast rate. This can be seen at the very low value of reacted fraction in the defined timeframe in Figure 5.

## Hydrogen release

For the release of hydrogen from the adiabatic storage reactor, the chemical reactions for hydrogen- and heat storage have to be reversed and a temperature gradient in the opposite direction is necessary. For heat transfer, the temperature, at which the thermal energy is released, has to be higher than the magnesium hydride dehydrogenation temperature. Previous analytical [13] and numerical [15] investigations indicated that a water vapor pressure of 9 bar should be sufficient to drive the process by reaching a temperature level of around 340 °C. However, to the best of our knowledge, the hydration of MgO at that high pressure has not been investigated before. Hence, the temperature that can be achieved in the reactor during MgO hydration is of utmost interest.

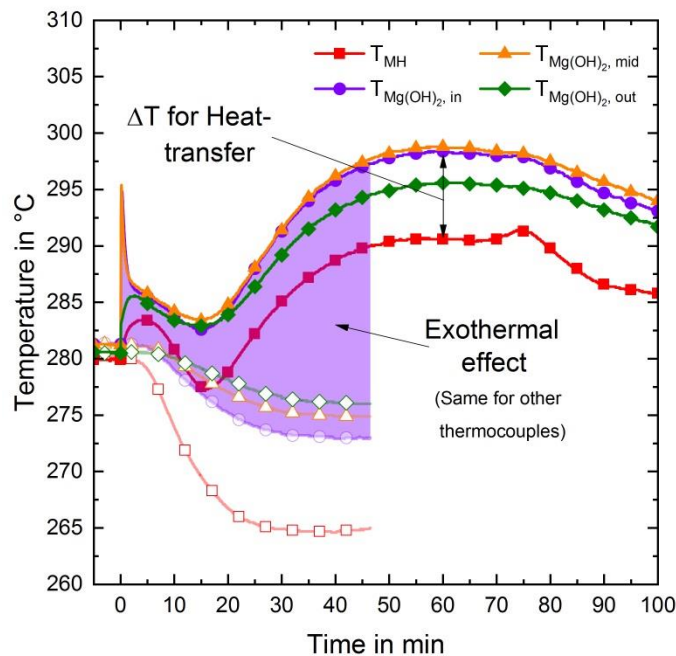


Figure 6 - Reactor temperatures during hydrogen release at 2.7 g h<sup>-1</sup>; 9.75 bar water vapor pressure (only full markers); Open markers: Reference experiment; Full markers: Combined experiment; Thermocouple positions in Figure 2.

Analogue to the hydrogen absorption, a reference experiment was conducted to evaluate the influence of the thermochemical heat storage reaction on the hydrogen release. During the reference experiment, no thermochemical heat was released. All thermal energy required for the dehydrogenation of magnesium hydride had to be taken from the environment, which results in a cooldown of the material. This behavior is shown in Figure 6. A hydrogen flow rate of 2.7 g h<sup>-1</sup> was applied and, thus, the magnesium hydride bed (red) cools down. For the reference experiment, the desired flow rate of 2.7 g h<sup>-1</sup> could be sustained for 19 minutes. Afterwards, it slowly starts to decline. For clarity, that curve is not shown in Figure 6. With reduced temperature, the reaction rate is reduced, which is why it levels off after approximately 30 min. The MgO bed cools down as well a little delayed, which is due to the thermal resistance of the set-up. Again, a temperature gradient can be observed in the MgO bed which is due to the position of the thermocouples in different depths, as shown in Figure 2.

In contrast, for the experiment with both reactions participating, the temperature profile is different. The process was initiated by opening a valve between the evaporator and the reactor. Again, at the same time, the outflow of hydrogen at  $2.7 \text{ g h}^{-1}$  was started. It can be seen, that the temperature course in the MgO exhibits a sharp peak in the beginning. Then, temperatures decrease until they start to increase to a maximum. The temperature in the magnesium hydride follows that trend. The initial spike in the MgO temperature is probably attributed to adsorption of water vapor on the material surface, but not to the hydration reaction [21]. From the subsequent temperature course it can be deduced that the exothermal hydration accelerates at approximately 15 min. The maximum temperature that could be achieved at a water vapor pressure of 9.75 bar is  $298.7 \text{ }^\circ\text{C}$ . This temperature is lower than expected, but high enough for heat transfer to the  $\text{MgH}_2$  bed, because its dehydrogenation is able to happen below that temperature. In contrast to the reference experiment, the desired hydrogen mass flow rate of  $2.7 \text{ g h}^{-1}$  could be sustained for 83 minutes before it starts to decline.

This maximum temperature achieved during MgO hydration is probably not the chemical equilibrium temperature at that pressure, but an effective equilibrium including thermal losses to the environment.. Nevertheless, this temperature is way lower than estimated analytically [13] and numerically [15] before. Extrapolation of equilibrium data obtained at pressures below 1 bar predicts a chemical equilibrium of  $348 \text{ }^\circ\text{C}$  at 9.7 bar [21]. It is well-known that the reaction system of  $\text{Mg(OH)}_2 / \text{MgO}$  – just as many other gas-solid reactions – can exhibit a different equilibrium temperature at a given pressure for hydration and dehydration, respectively, which is known as hysteresis [22]. Since this influences the maximum temperature for the heat release, it was clear that it may affect the storage reactor's performance significantly, but so far it was not known at such high pressures of 9 bar. Concluding from the present experiments, it can be stated that even though the reaction system exhibits this significant hysteresis, the system is able to provide heat at a sufficiently high temperature to release the previously stored hydrogen.

#### Influence of MgO Hydration pressure on the hydrogen release

The adiabatic storage reactor's main advantage is its combination of two independently controllable thermochemical gas-solid reactions. In comparison to similar concepts, such as the usage of a PCM [7], the advantage is that the temperature level at which heat is released or stored, can be adjusted with the gas pressure of the water vapor. Hence, gas pressure has an important influence on the reaction system. Figure 7 shows the influence of the water vapor pressure on the MgO hydration, which is the exothermal release of the previously stored thermal energy required for the hydrogen release. The initial temperature spike, which is probably attributed to adsorption, does not increase the reacted fractions. Even though the water vapor pressure has only been raised by 300 mbar from 9.45 bar to 9.75 bar, an increase in the maximum temperature is obvious - compare Figure 7 (A). The maximum temperature reached in the MgO bed increases from  $295 \text{ }^\circ\text{C}$  to  $298 \text{ }^\circ\text{C}$ . This leads to a higher temperature in the magnesium hydride bed, where the  $\text{H}_2$  release reaction can be sustained longer at the given rate, as it can be seen in Figure 7 (B). Additionally, this small increase in gas pressure accelerates the MgO hydration rate which can also be seen in Figure 7 (B).

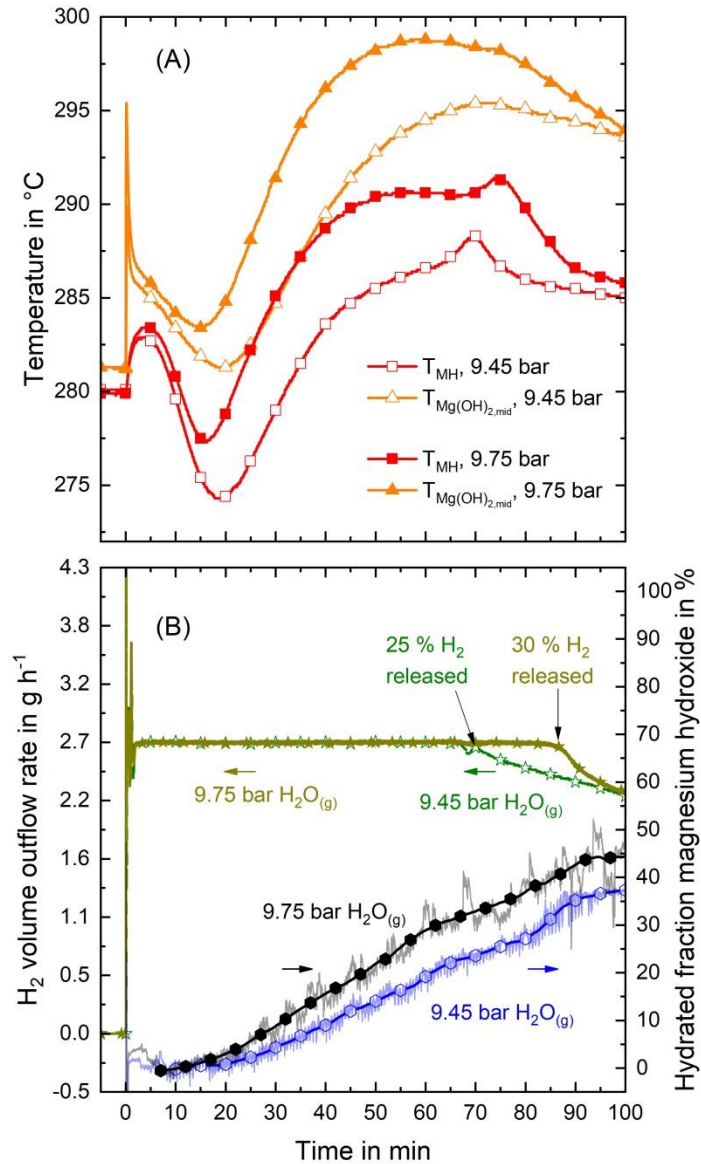


Figure 7 - Influence of MgO hydration pressure; Hydrogen outflow rate  $2.7\ g\ h^{-1}$ ; Full markers: 9.75 bar; Open Markers: 9.45 bar.

Similar to the hydrogen storage process, thermal losses occur during the hydrogen release in the present system. As long as the temperature in the reactor is higher than the initial temperature, there is a temperature gradient to the ambient leading to thermal losses. This is the case for most of the time, as it can be seen in Figure 7 (A). Compared to the hydrogen storage process (Figure 3), however, the temperature level of the exothermal reaction is 60 K lower. Therefore, the temperature gradient to the environment is lower and thermal losses are less pronounced. This can be seen in the values for the conversion in Figure 7 (B). For the 9.45 bar case, 25% of the stored hydrogen was released and 24% of the MgO hydrated at 70 min. Similarly, for the 9.75 bar case, 30% Hydrogen is released with 39% conversion in the MgO reaction at 85 min. Therefore, it can be concluded that the released heat during MgO hydration is being consumed by the  $MgH_2$  dehydrogenation, rather than being lost to the environment. The

experiment was stopped before 100% of the materials reacted since the hydrogen release rate started to decline rapidly, as it can be seen in Figure 7 (B).

### Influence of operating mode on hydrogen release

Depending on the application, it may be a matter of interest to withdraw hydrogen from the reactor at a constant pressure or a constant mass flow rate. At a constant pressure, the reactor would operate at

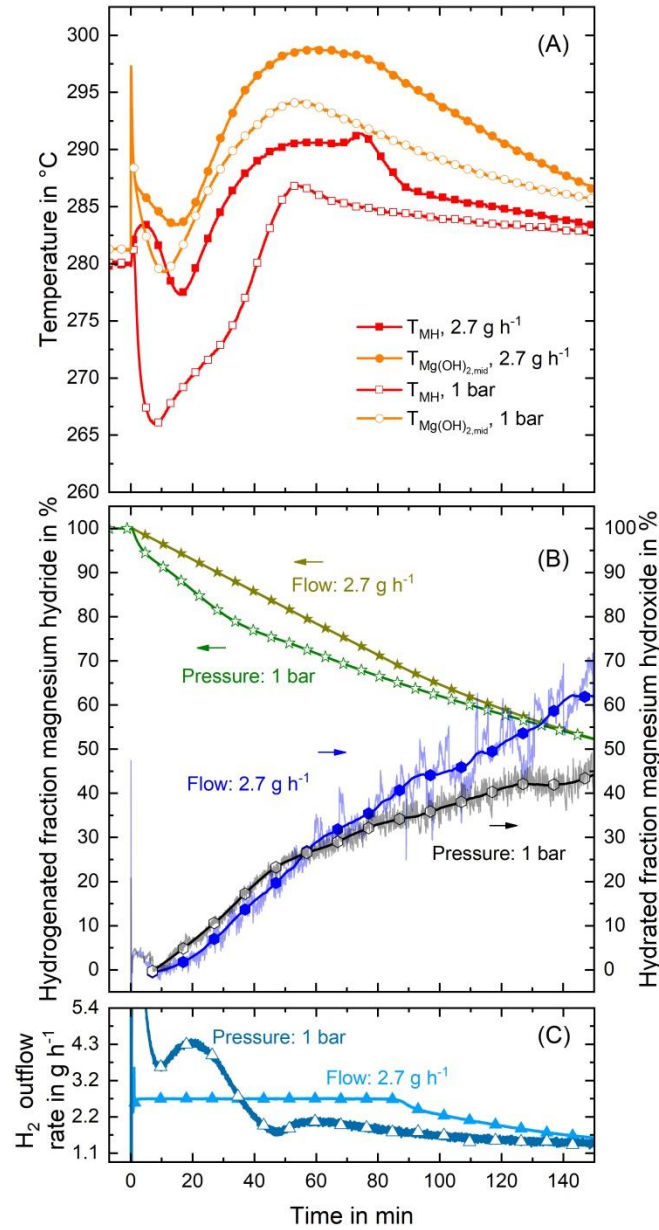


Figure 8 – Influence of operation mode maximum power or constant power; MgO hydration pressure: 9.75 bar; Full markers: Constant power at  $2.7 \text{ g h}^{-1}$   $H_2$  flow; Open markers: Maximum power at 1 bar  $H_2$  pressure.

maximum power while it would be at constant power during the operating mode of constant mass flow rate. The comparison between the two modes at a pressure of 1 bar and  $2.7 \text{ g h}^{-1}$ , respectively, is shown in Figure 8. The initial conditions are similar. It can be seen that the temperature in the maximum power case decreases rapidly since dehydrogenation is taking place consuming thermal energy from the materials. This initial temperature drop decreases the temperature level of the whole process, which is evident in Figure 8 (A). Subsequently, more hydrogen is released initially as it can be seen in Figure 8 (C). Therefore, the hydration of MgO happens at a lower temperature and results in slower reaction rate. This can be seen in Figure 8 (B) since the hydrated fraction is lower after 140 min.

Therefore it can be concluded here, that hydrogen can be withdrawn at maximum – or constant power. However, if the temperature in the reactor drops too low, the MgO hydration reaction is not able to deliver enough heat to maintain the maximum power because the bed cools down thereby reducing the reaction rate. Thus, if not operated carefully, the present adiabatic storage reactor is able to impede itself during hydrogen release since the reaction rates are sensitive to the temperature in the chosen conditions.

#### Influence of the temperature level on the MgO hydration

As it was discussed in the previous sections, the thermochemical heat storage reaction is the limiting factor in the present setup. During the hydrogen release process, rapid release of thermal energy would result in rapid hydrogen release. Little is known about the exothermal reaction of magnesium oxide with water vapor at such high pressures of more than 9 bar. Therefore, the initial temperature of the hydrogen release was varied for hydration at 9.75 bar and a hydrogen flow rate of  $2.7 \text{ g h}^{-1}$ . Figure 9 (A) and (B) show the temperature course in the MgO bed and the reacted fractions of the MgO, respectively. In all cases, the temperature drops in the beginning before it starts to increase again. The beginning of this increase occurs earlier for lower temperatures and later for higher temperatures. Apart from that, in the  $281 \text{ }^\circ\text{C}$  and the  $266 \text{ }^\circ\text{C}$  cases the temperature courses are almost identical, just shifted for 15 K. Additionally, for the  $296 \text{ }^\circ\text{C}$  case, the temperature course is more flat.

The increase of temperature after the minimum indicates that the exothermal MgO hydration reaction starts to accelerate. This can be confirmed with Figure 9 (B), since the increase in temperature coincides with the increase in reacted fractions. According to Arrhenius's law, a reaction rate increases with increasing temperature, however, this behavior cannot be observed here. Instead, at higher temperatures the reaction starts to accelerate later and less pronounced. Therefore, it can be concluded that the chemical equilibrium is approached at the higher temperature which reduces the driving force, and thus, the reaction rate of the chemical reaction. Since the maximum temperature archived is different as well, it can be concluded that the reaction is hindered kinetically due to the proximity of the equilibrium. Otherwise, the maximum of the temperature achieved would be the same for all cases.

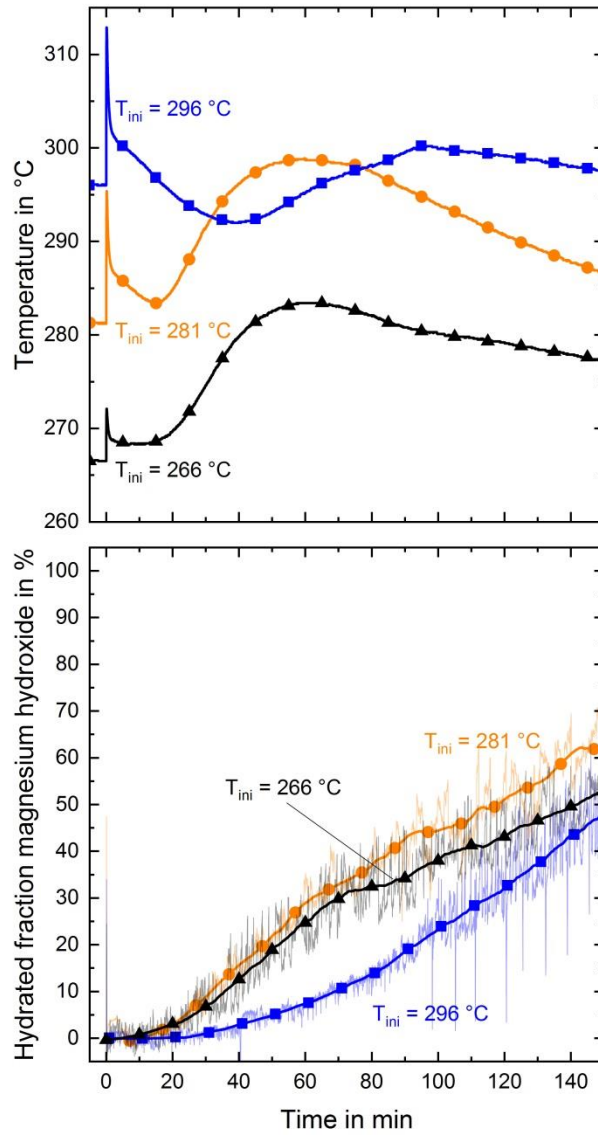


Figure 9 - Influence of initial temperature on MgO hydration; MgO hydration pressure: 9.75 bar; Hydrogen outflow rate: 2.7 g h<sup>-1</sup>; Shown Thermocouple: T<sub>Mg(OH)<sub>2</sub>, mid</sub>.

From the fact that the maximum temperature is approximately the same for the medium and high initial temperature, it can be concluded that the maximum possible temperature to be reached in this setup is around 300 °C.

## Optimization approaches

The present prototype reactor was designed to proof the hydrogen storage and release capability of this adiabatic system and that the necessary temperature gradients can be established. The reactor design did not aim for high storage density, to minimize hydrogen storage/release times, to fully utilize the materials involved or to investigate the cycling behavior. The present non-optimized prototype exhibits a gravimetric and volumetric hydrogen density of approximately  $0.40 \text{ g}_{\text{H}_2} \text{ kg}^{-1}$  and  $0.20 \text{ g}_{\text{H}_2} \text{ L}^{-1}$ , respectively. These values include the prototype reactor's steel vessel, flanges, insulation and reactive materials assuming 100% hydrogenation of the metal hydride. Assuming 100% conversion for the magnesium hydride pellets and 80% conversion of the  $\text{Mg}(\text{OH})_2$  powder (Porosity 62%) and regarding only the volume of the two reactive materials, a volumetric density of  $20.8 \text{ g}_{\text{H}_2} \text{ L}^{-1}$  can be achieved. The value of a real system in large scale will be a little lower, since the steel for the reactor and the insulation has to be taken into account. The amount of steel is depending on the overall reactor design and is not deducible from the prototype reactor. As the steel required for that purpose will add weight to the system but only little in volume and the insulation has to be applied on the reactor's exterior only, the comparison with other systems is justified. Operating below 10 bar, the volumetric storage density of the adiabatic storage reactor exceeds state of the art hydrogen storage in compressed tanks at 350 bar ( $16.1 \text{ g}_{\text{H}_2} \text{ L}^{-1}$ ) and is approximately equal to 700 bar compressed tanks ( $21\text{-}26 \text{ g}_{\text{H}_2} \text{ L}^{-1}$ ) [17]. Material modifications may increase the storage density of the adiabatic storage reactor to up to  $25 \text{ g}_{\text{H}_2} \text{ L}^{-1}$  which is at the upper end of the 700 bar pressure tank range. However, there is room for optimization, for example in the following suggestions.

First, the volumetric storage density of the storage reactor can be enhanced by compressing the thermochemical heat storage material to pellets with higher density and less porosity compared to a fine powder, similar to the magnesium hydride pellets. Second, the experimental results revealed a kinetic limitation of the  $\text{Mg}(\text{OH})_2 / \text{MgO}$  reaction system which has been used as thermochemical heat storage material. Improving the reaction rates will lead to faster heat storage/release and subsequent faster hydrogen storage/release. Therefore, the material should be modified or doped, which already is a research topic [23] [24].

Third, the prototype reactor designed in this work exhibits thermal losses, which means that released heat of the exothermal reaction is not being fully consumed by the other endothermal reaction. Instead, the heat is partially lost to the environment. Therefore, the reaction rate of the exothermal reaction is faster than the endothermal reaction rate, resulting in uneven conversions. For the adiabatic system to work reversibly, the heat of absorption has to be fully consumed by the thermochemical heat storage reaction. Otherwise the heat is not available for the hydrogen release. Since the prototype is only a single tube, thermal losses were expected. In a larger system thermal losses can be lower, since the surface-to-volume ratio can be reduced. Thermal losses in the present setup occurred mainly at the surface of the prototype reactor. Therefore, matching conversions can be expected in large scale applications.

The cost of the proposed adiabatic storage reactor in large scale is difficult to determine, since it depends strongly on the design of the reactor and its surrounding infrastructure. The cost of the presented prototype exceeds any economic feasibility by far. However, the raw materials of the proposed system only require magnesium which can be obtained for  $2\text{-}3 \text{ USD kg}_{\text{Mg}}^{-1}$  [25]. Therefore, the lower threshold for the material cost is  $52\text{-}78 \text{ USD kg}_{\text{H}_2}^{-1}$ . This is a prerequisite for large scale application.

## Conclusion

In this work the experimental proof of concept of a novel hydrogen storage concept was demonstrated. It utilizes two thermochemical reactions for hydrogen storage and heat storage, respectively. Magnesium hydride ( $\text{MgH}_2$ ) is used for hydrogen storage and the  $\text{Mg(OH)}_2$  /  $\text{MgO}$  system for heat storage. Hence, an exothermal reaction is coupled with an endothermal one compensating for each other. Due to the high hydrogen storage capacity of  $\text{MgH}_2$ , the storage concept exhibits high storage densities at low pressures below 10 bar. The materials used are non-toxic, cheap and abundantly available. Therefore, this storage technology may be a part of a hydrogen economy in the future. A lab scale reactor prototype was developed and characterized. Even though there is potential for optimization during upscaling, the working principle has been proofed. The thermochemical properties of the materials fit to each other for both hydrogen storage and release. Facing thermal losses and poor kinetics of the  $\text{Mg(OH)}_2$ / $\text{MgO}$  system, 100% conversion was not achieved with simultaneous thermochemical cooling/heating during hydrogen storage/release, respectively. However, it has been demonstrated that hydrogen can be stored at a high volumetric capacity at a pressure below 10 bar, which makes the adiabatic storage reactor a promising option for stationary hydrogen storage. For hydrogen release, the previously stored heat has to be released. It has been shown that the hydration of  $\text{MgO}$  at a water vapor pressure of 10 bar results in a temperature level of 300 °C, which has never been experimentally investigated before. This temperature is sufficiently high to drive the  $\text{MgH}_2$  dehydrogenation in the present system.

## Acknowledgments

The authors want to thank the Karl-Vossloh-Stiftung (Project No.: S047/10043/2017) for partially funding this work.

## Bibliography

- [1] A. Lewandowska-Bernat and U. Desideri, "Opportunities of power-to-gas technology in different energy systems architectures," *Applied Energy*, vol. 228, pp. 57-67, 2018.
- [2] T. Maeda, K. Nishida, M. Tange, T. Takahashi, A. Nakano, H. Ito, Y. Hasegawa, M. Masuda and Y. Kawakami, "Numerical simulation of the hydrogen storage with reaction heat recovery using metal hydride in the totalized hydrogen energy utilization system," *International Journal of Hydrogen Energy*, vol. 36, no. 17, pp. 10845-10854, 2011.
- [3] The High Pressure Gas Safety Institute of Japan (KHK), "<https://www.khk.or.jp/english>," [Online]. Available: [https://www.khk.or.jp/Portals/0/resources/english/dl/hpgact\\_overview.pdf](https://www.khk.or.jp/Portals/0/resources/english/dl/hpgact_overview.pdf). [Accessed 12 09 2019].
- [4] B. Sakintuna, F. Lamari-Darkrim and M. Hirscher, "Metal hydride materials for solid hydrogen storage: a review," *International journal of hydrogen energy*, vol. 32, no. 9, pp. 1121-1140, 2007.
- [5] M. Yadav and Q. Xu, "Liquid-phase chemical hydrogen storage materials," *Energy & Environmental Science*, vol. 5, no. 12, pp. 9698-9725, 2012.
- [6] S. Niaz, T. Manzoor and A. H. Pandith, "Hydrogen storage: Materials, methods and perspectives," *Renewable and Sustainable Energy Reviews*, vol. 50, pp. 457-469, 2015.
- [7] S. Garrier, B. Delhomme, P. De Rango, P. Marty, D. Fruchart and S. Miraglia, "A new MgH<sub>2</sub> tank concept using a phase-change material to store the heat of reaction," *International Journal of Hydrogen Energy*, vol. 38, no. 23, pp. 9766-9771, 2013.
- [8] S. Mellouli, N. Ben Khedher, F. Askri, A. Jemni and S. Ben Nasrallah, "Numerical analysis of metal hydride tank with phase change material," *Applied Thermal Engineering*, vol. 90, pp. 674-682, 2015.
- [9] S.-K. Seo, D.-Y. Yun and C.-J. Lee, "Design and optimization of a hydrogen supply chain using a centralized storage model," *Applied Energy*, vol. 262, p. 114452, 2020.
- [10] G. Alva, Y. Lin and G. Fang, "An overview of thermal energy storage systems," *Energy*, vol. 144, pp. 341-378, 2018.
- [11] V. Yartys, M. Lototskyy, E. Akiba, R. Albert, V. Antonov, J. Ares, M. Baricco, N. Bourgeois, C. Buckley, J. B. von Colbe, J.-C. Crivello, F. Cuevas, R. Denys, M. Dornheim, M. Felderhoff, D. Grant, B. Hauback, T. Humphries, I. Jacob, T. Jensen, P. de Jongh, J.-M. Joubert, M. Kuzovnikov, M. Latroche,

- M. Paskevicius, L. Pasquini, L. Popilevsky, V. Skripnyuk, E. Rabkin, M. Sofianos, A. Stuart, G. Walker, H. Wang, C. Webb and M. Zhu, "Magnesium based materials for hydrogen based energy storage: Past, present and future," *International Journal of Hydrogen Energy*, vol. 44, no. 15, pp. 7809-7859, 2019.
- [12] T. Sadhasivam, H.-T. Kim, S. Jung, S.-H. Roh, J.-H. Park and H.-Y. Jung, "Dimensional effects of nanostructured Mg/MgH<sub>2</sub> for hydrogen storage applications: a review," *Renewable and Sustainable Energy Reviews*, vol. 72, pp. 523-534, 2017.
- [13] M. Bhourri, I. Bürger and M. Linder, "Feasibility analysis of a novel solid-state H<sub>2</sub> storage reactor concept based on thermochemical heat storage: MgH<sub>2</sub> and Mg (OH)<sub>2</sub> as reference materials," *International Journal of Hydrogen Energy*, vol. 41, no. 45, pp. 20549-20561, 2016.
- [14] M. Bhourri and I. Bürger, "Numerical investigation of H<sub>2</sub> absorption in an adiabatic high-temperature metal hydride reactor based on thermochemical heat storage: MgH<sub>2</sub> and Mg (OH)<sub>2</sub> as reference materials," *International Journal of Hydrogen Energy*, vol. 42, no. 26, pp. 16632-16644, 2017.
- [15] M. Lutz, M. Bhourri, M. Linder and I. Bürger, "Adiabatic magnesium hydride system for hydrogen storage based on thermochemical heat storage: Numerical analysis of the dehydrogenation," *Applied energy*, vol. 236, pp. 1034-1048, 2019.
- [16] Multi, "Annual Work Plan 2014 - 2020 of the FCH JU," [Online]. Available: [https://www.fch.europa.eu/sites/default/files/MAWP%20final%20version\\_endorsed%20GB%2015062018%20%28ID%203712421%29.pdf](https://www.fch.europa.eu/sites/default/files/MAWP%20final%20version_endorsed%20GB%2015062018%20%28ID%203712421%29.pdf).
- [17] M. Hirscher and K. Hirose, *Handbook of Hydrogen Storage: New Materials for Future Energy Storage*, Weinheim: John Wiley & Sons, 2010, p. 13.
- [18] J. O. Jensen, A. P. Vestbø, Q. Li and N. Bjerrum, "The energy efficiency of onboard hydrogen storage," *Journal of Alloys and Compounds*, Vols. 446-447, pp. 723-728, 2007.
- [19] M. Schmidt, C. Szczukowski, C. Roßkopf, M. Linder and A. Wörner, "Experimental results of a 10 kW high temperature thermochemical storage reactor based on calcium hydroxide," *Applied Thermal Engineering*, vol. 62, no. 2, pp. 553-559, 2014.
- [20] C. Pohlmann, L. Röntzsch, S. Kalinichenka, T. Hutsch, T. Weißgärber and B. Kieback, "Hydrogen storage properties of compacts of melt-spun Mg<sub>90</sub>Ni<sub>10</sub> flakes and expanded natural graphite," *Journal of Alloys and Compounds*, vol. 509, pp. S625-S628, 2011.
- [21] Y. Kato, N. Yamashita, K. Kobayashi and Y. Yoshizawa, "Kinetic study of the hydration of magnesium oxide for a chemical heat pump," *Applied Thermal Engineering*, vol. 16, no. 11, pp. 853-862, 1996.

- [22] S. Kiyabu, J. S. Lowe, A. Ahmed and D. J. Siegel, "Computational Screening of Hydration Reactions for Thermal Energy Storage: New Materials and Design Rules," *Chemistry of Materials*, vol. 30, no. 6, pp. 2006-2017, 2018.
- [23] A. I. Shkatulov and Y. Aristov, "Thermochemical Energy Storage using LiNO<sub>3</sub>-Doped Mg (OH) <sub>2</sub>: A Dehydration Study," *Energy Technology*, vol. 6, no. 9, pp. 1844-1851, 2018.
- [24] A. Shkatulov, H. Takasu, Y. Kato and Y. Aristov, "Thermochemical energy storage by LiNO<sub>3</sub>-doped Mg (OH) <sub>2</sub>: Rehydration study," *Journal of Energy Storage*, vol. 22, pp. 302-310, 2019.
- [25] H. Shao, L. He, H. Lin and H.-W. Li, "Progress and Trends in Magnesium-Based Materials for Energy-Storage Research: A Review," *Energy Technology*, vol. 6, no. 3, pp. 445-458, 2018.